Phys Chem Minerals (2013) 40:11–17
DOI 10.1007/s00269-012-0541-9

ORIGINAL PAPER

Electrical conductivity of talc aggregates at 0.5 GPa: influence of dehydration

Duojun Wang · Shun-ichrio Karato

Received: 29 March 2012 / Accepted: 13 September 2012 / Published online: 26 September 2012

Abstract Electrical conductivity of talc was measured at 0.5 GPa and ~473 to ~1,300 K by using impedance spectroscopy both before and after dehydration. Before dehydration, the electrical conductivity of talc increased with temperature and is $\sim 10^{-4}$ S/m at 1,078 K. After dehydration, most of the talc changed to a mixture of enstatite and quartz and the total water content is reduced by a factor 6 or more. Despite this large reduction in the total water content, the electrical conductivity increased. The activation enthalpy of electrical conductivity (~125 kJ/mol) is too large for the conduction by free water but is consistent with conduction by small polaron. Our results show that a majority of hydrogen atoms in talc do not enhance electrical conductivity, implying the low mobility of the hydrogen atoms in talc. The observed small increase in conductivity after dehydration may be attributed to the increase in oxygen fugacity that enhances conductivity due to small polaron.

Keywords Talc · Dehydration · Electrical conductivity

Introduction

Seismic and electromagnetic anomalies have been observed in some subduction zones (Matsuzawa et al. 1986; Helffrich and Abers 1997; Kawakatsu and Watada 2007; Kurtz et al. 1990; Ichiki et al. 2009). These anomalies (high conductivity and low seismic wave velocities) are often interpreted as due to hydrous minerals (Ichiki et al. 2009; Kawakatsu and Watada 2007).

Hydrous minerals carry a large amount of water (a few wt%), and therefore, it would be important if one can infer the distribution of hydrous minerals from geophysical observations. Hydrous minerals in general have low seismic wave velocities compared to anhydrous counter parts (Ito 1990; Ito and Tatsumi 1995; Bailey and Holloway 2000), and this can be interpreted as due to the weak chemical bonds involving hydrogen. In contrast, the electrical conductivity of hydrous minerals is not always high (e.g., Reynard et al. 2011; Guo et al. 2011). However, there is a large scatter in the published results on the electrical conductivity of hydrous minerals, and it is important to investigate this issue in more detail.

In this paper, we studied the electrical conductivity of talc. Talc is a hydrous magnesium silicate in the subduction zone; it may sink into ~60 km (Ulmer and Trommsdorff 1999). In addition, talc in the crust may break down in the vicinity of volcanic arc and release water (Peacock and Hyndman 1999; Peacock 2001; Ranero et al. 2003). Therefore, the influence of dehydration of talc on the electrical conductivity is also important. Consequently, we measured the electrical conductivity both before and after the dehydration reaction.

Water (hydrogen) can enhance the electrical conductivity in nominally anhydrous minerals (NAMs) due to the higher mobility of charged carriers (e.g., Karato 1990; Wang et al. 2006; Yang et al. 2011). Consequently, hydrous minerals, containing higher water (hydrogen) concentration than those of nominate anhydrous mineral (NAMs), might be expected to account for the extremely

D. Wang (✉)
Key Laboratory of Computational Geodynamics,
Graduate University of Chinese Academy of Sciences,
Beijing 100049, China
e-mail: duojunwang@hotmail.com

S. Karato
Department of Geology and Geophysics,
Yale University, New Haven, CT, USA

high (~0.1–1 S/m) electrical conductivity from geophysical results (e.g., Ichiki et al. 2009). To address this issue, laboratory studies on electrical conductivity and thermal dehydration of hydrated minerals such as talc and amphibole are required.

Many attentions (Bose and Ganguly 1994; Liao and Senna 1992; Wesolowski and references therein 1984) were paid to study thermal dehydration of talc. In contrast, so far a few studies (Zhu et al. 2001; Guo et al. 2011) on the electrical conductivity of talc have been performed. However, discrepancies have been found both in the absolute values of electrical conductivity and the activation enthalpy in the previous studies (Zhu et al. 2001; Guo et al. 2011). Zhu et al. (2001) measured the electrical conductivity of talc at $P = 1.0$, 2.0 GPa and at 673–1,033 K and show electrical conductivity is up to 1 S/m at ~1,033 K. They demonstrated that dehydration of talc weakly affected the electrical conductivity. However, Zhu et al. (2001) did not check the water content before and after electrical conductivity measurement as well as the product after experiment. Guo et al. (2011) measured the anisotropy of the electrical conductivity of talc at 3.0 GPa at 500–1,000 K, but they did not pay attention to the dehydration effect on the electrical conductivity. In contrast, the electrical conductivity of talc from Guo et al. (2011) is two orders of magnitude lower than that of previous study from Zhu et al. (2001). The activation enthalpy of ~250 kJ/mol obtained by Zhu et al. (2001) is larger than the results (56–64 kJ/mol) from Guo et al. (2010). In addition, so far the influence of dehydration on electrical conductivity has not been studied in any detail which is critical to the understanding of the electrical conductivity anomalies.

In this study, we report the results of electrical conductivity measurements of talc before and after dehydration at high pressure. In addition to electrical conductivity measurements, we have characterized samples using FTIR, Raman, and X-ray diffraction before and after dehydration.

Experimental procedure

The sample

The starting material was natural talc polycrystalline aggregates with the white color from China (locality is unknown). The chemical compositions were analyzed by the X-ray fluorescence (shown in Table 1), which is close to the pure talc. Figure 1 shows the back-scattered electron (BSE) images both before (Fig. 1a) and after experiment (Fig. 1b). Two new phases including enstatite and quartz are observed after dehydration.

Table 1 The chemical compositions of talc determined by X-ray fluorescence

	Talc
SiO_2	62.35
TiO_2	0.01
Al_2O_3	0.10
Cr_2O_3	0.08
FeO	0.51
MnO	0.00
MgO	31.31
CaO	0.08
Na_2O	0.01
K_2O	0.05
P_2O_5	0.04
LoI	5.74
Total	100.20

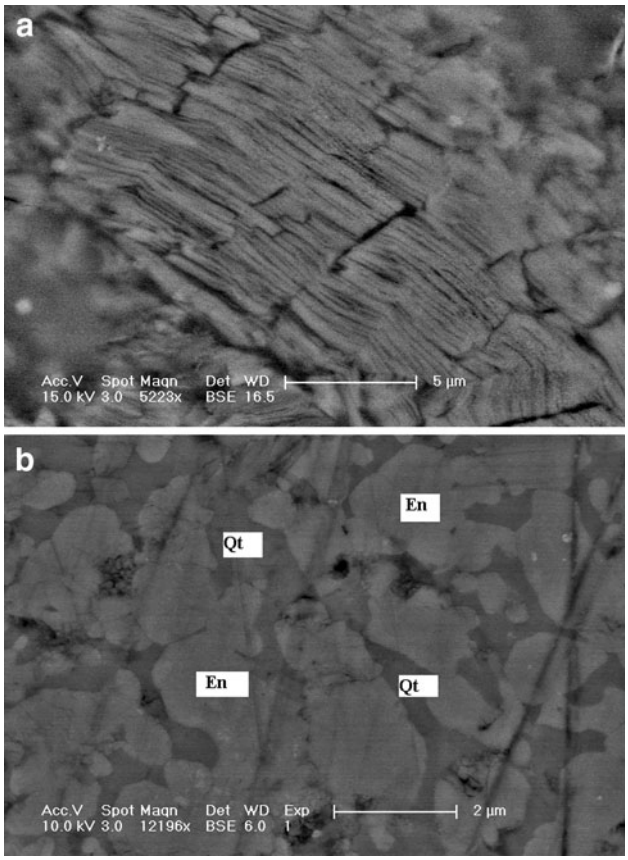

Fig. 1 The back-scattered electron (BSE) images of talc before (**a**) and after (**b**) electrical conductivity measurement. *Qt* quartz, *En* estatite

Experimental method

The high-pressure experiments were conducted by using a cubic-anvil high-pressure apparatus, described in detail elsewhere (Wang et al. 2010, 2012; Guo et al. 2010). The cubic-shaped pyrophyllite (32 mm × 32 mm × 32 mm) sintered at 1,173 K was used as the pressure medium where

the pressure was generated by six tungsten-carbide square-surface anvils. In the sample assembly, an Al_2O_3 insulating tube was placed at the center of the heater to insulate the sample from the heater. The furnace was made of three layers of stainless steel foils. The sample was sandwiched by the Ni electrodes. The sample has a disk shape with a thickness of ~4.5 mm and a diameter of 8.0 mm. The temperatures were monitored by a NiCr–NiAl (K-type) thermocouple placed against the sample.

Complex impedance measurements were performed at 0.5 GPa confining pressure, using a Solartron 1260 impedance phase analyzer. A 1-V sinusoidal signal was applied in the frequency range ~100–10^6 Hz for the high temperature and pressure experiments. The complex impedance was measured in three heating–cooling cycles at a given pressure. Measurements were taken from ~473 to ~1,300 K. An equivalent circuit composed of a resistor in parallel with a capacitor was used to determine the resistance of the samples at certain temperature at a given pressure.

Results

Figure 2 shows the representative electrical impedance spectra across the dehydration temperature—both heating and cooling cycles in the form of complex plane plots (real part Z') versus imaginary part (Z''). The complex impedance of the sample shows the negative Z'' and positive Z' in most cases corresponding to the equivalent circuit of a parallel combination of a resistor and a capacitor (e.g., Roberts and Tyburczy 1991; Huebner and Dillenburg 1995). The capacitive arc in the high frequency range from 10^3 to 10^6 Hz corresponding to the resistor of the sample was used to calculate the electrical conductivity. However, at low frequencies and at high temperatures, the impedance spectroscopy observations show the positive Z'' indicative of the presence of inductive component. Previous studies (Macdonald 1978; Bai and Conway 1991) indicated that the inductive behavior in the low frequency is attributed to the chemical reaction at the sample electrode interface. Thus, the inductive loop at low frequency indicated that the dehydration reaction occurred and the Ni was oxidized to NiO.

The results of electrical conductivity derived from impedance arc at the high frequency range of ~10^3–10^6 Hz at various temperatures were shown in Fig. 3. Three heating and cooling cycles were carried out during all the electrical conductivity measurements. In the first and the second cycles, the sample was heated up to ~873 K and then was cooled to ~473 K. The conductivity values did not change much during these cycles except several data points at the lower temperatures. In the

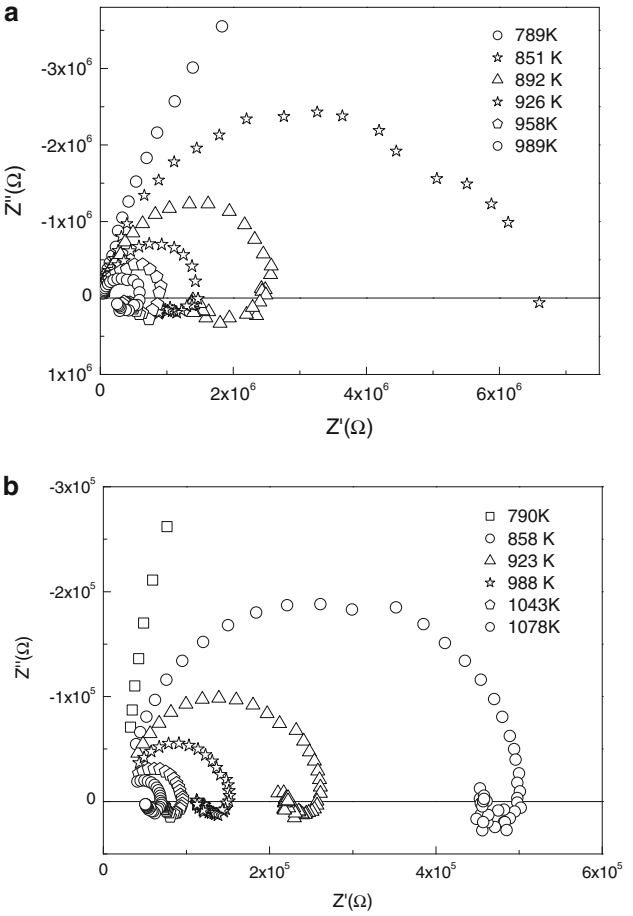

Fig. 2 Impedance spectrum of talc in third heating cycle (**a**) and in third cooling cycle (**b**). These *symbols* represent impedance arcs at different temperatures. The frequency of each point increases from *right* to *left* along each trajectory

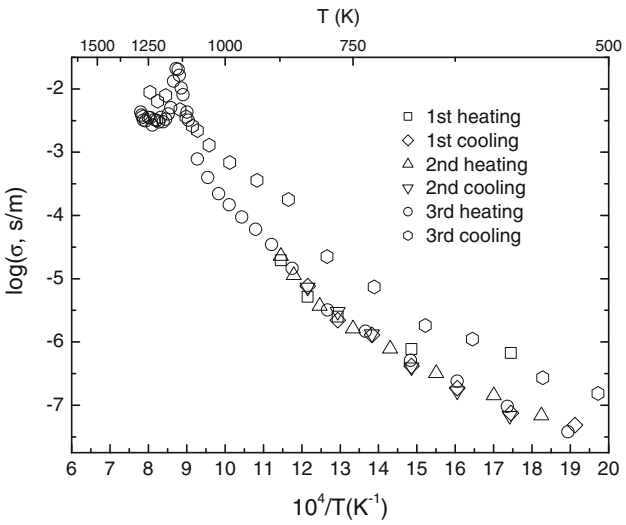

Fig. 3 Logarithm of electrical conductivity as a function of reciprocal temperature for talc in the three heating and cooling cycles at 0.5 GPa

Table 2 Fitting parameters for talc corresponding to Eq. 1

Temperature (K)	$\log_{10}A$ (S/m)	H^* (kJ/mol)
Before dehydration		
473–823	−2.42 ± 0.22	49 ± 3
823–1,078	3.18 ± 0.20	131 ± 4
After dehydration		
463–790	−1.37 ± 0.38	52 ± 4
858–1,183	3.42 ± 0.20	125 ± 4

third cycle, the sample was heated up to ~1,300 K and then was cooled to 423 K. In the third heating cycle, the conductivity values show good repeatability for the temperature range from 423 to 873 K. The slope change occurs around 840 and 890 K, suggesting that the conduction mechanism changes at around this temperature. In the third cooling cycle, the electrical conductivity values are slightly larger than those in the third heating cycles in the temperature range of 423–1,046 K.

The activation enthalpies were separately calculated by fitting the electrical data in the range of lower and higher temperatures, according to the following equation:

$$\sigma = A\exp(-H^*/RT) \quad (1)$$

where A, the pre-exponential factor and H^*, the activation enthalpy are experimentally determined quantities. R is the gas constant, and T is temperature. The fitting parameters are listed in Table 2.

FTIR spectra before and after electrical conductivity measurements of talc were shown in Fig. 4. It can be seen that the absorption peaks decreased significantly (by a factor of 6 or more) after the electrical conductivity measurement when the maximum temperature exceeds 1,300 K.

The Raman spectra before and after the conductivity measurement of talc compared with the Raman spectra of orthopyroxene and quartz were shown in Fig. 5. It can be seen that two peaks appear at ~342 and 679 cm^{-1} before the electrical conductivity measurement, while after the electrical conductivity measurement, the two new double peaks appear at 661–679 cm^{-1} corresponding to enstatite, and a new peak at 460 cm^{-1} corresponds to SiO_2.

The X-ray diffraction (XRD) was used to identify the phases both before and after EC measurement, and enstatite and quartz are found, and this agrees well with that of Raman spectra.

Discussion and conclusion

The electrical conductivity of talc shows four stages at the temperature range of 473–1,300 K. Before dehydration from 473 to 823 K, electrical conductivity is characterized

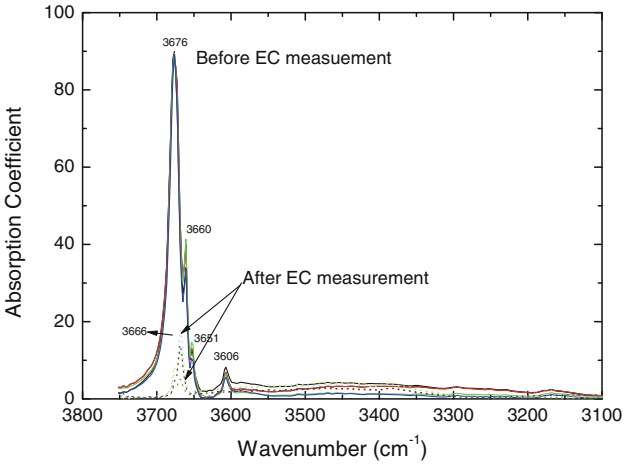

Fig. 4 FTIR spectra of talc before and after electrical conductivity measurement. *Solid* and *dashed lines* represent the FTIR spectra of talc before and after measurements, respectively

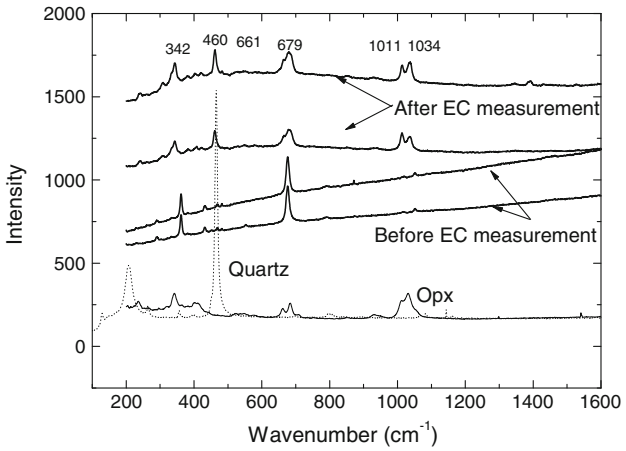

Fig. 5 Raman spectra of talc before and after EC measurement, enstatite, and quartz

by a small activation enthalpy (49 kJ/mol), and activation enthalpy is larger (130 kJ/mol) from 823 to 1,078 K. From 1,106 to 1,300 K (during dehydration), the conductivity behavior is complicated but increases by an order of magnitude in the narrow temperature range. After dehydration, the electrical conductivity is higher than that before dehydration (at the same temperature) with the activation enthalpies (125 and 52 kJ/mol) similar to those before dehydration. During the third heating to 1,023 K, talc may enter into the anthophyllite + quartz + H_2O stability (Evans and Guggenheim 1988) field; thus, the temperature dependence of conductivity across these transitions might include the influence of these transformations. This transition may factor into the change in activation enthalpy above 873 K. The activation enthalpy (~50 kJ/mol) at low temperature is similar to that obtained Guo et al. (2011) that conduction mechanism in this

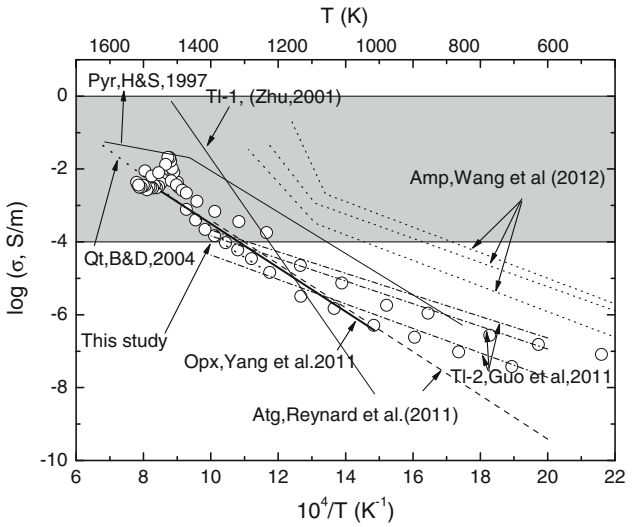

Fig. 6 A comparison of the results on electrical conductivity of the various minerals. Opx is the electrical conductivity of orthopyroxene reported by Yang et al. (2011) whose iron content was normalized to the same value as talc used in this study. Pyr is the electrical conductivity of pyrophyllite reported by Hicks and Secco (1997); Atg represents the electrical conductivity of antigorite given by Reynard et al. (2011); Tl-1 is the electrical conductivity of talc by Zhu et al. (2001); Tl-2 represents the electrical conductivity of talc in the direction of *X*, *Y*, and *Z* (from *top* to *bottom*), respectively, which is reported by Guo et al. (2011). Amp corresponds to the electrical conductivity of amphibole-bearing rocks reported by Wang et al. (2012)

temperature range is likely due to free proton. However, the high activation enthalpy (~125 kJ/mol) has not been reported yet.

The increase in electrical conductivity of sample in the temperature range of 1,106–1,155 K may reflect the dehydration of talc where more than 80 % water (hydrogen) released (Fig. 4). As a result of dehydration, new phases were formed (Figs. 1, 5) as confirmed by SEM as well as the Raman spectroscopy and XRD. The process of dehydration of talc to form enstatite can be described by the following reaction:

$$Mg_6Si_8O_{20}(OH)_4 \rightarrow 6MgSiO_3 + 2SiO_2 + 2H_2O$$

The FTIR measurements of a sample after dehydration showed that a majority of water (hydrogen) released by dehydration was largely removed from the system. Also, the activation enthalpy of electrical conductivity after dehydration (125 kJ/mol) is much larger than that of aqueous fluids (Gaillard 2004), and we believe that free water did not contribute much to electrical conductivity measurements.

In Fig. 6, we compared the electrical conductivity of talc both before and after dehydration with those of quartz (Bagdassarov and Delépine 2004) and orthopyroxene (Yang et al. 2011). The electrical conductivity of quartz with random orientations is controlled by alkali ions (Bagdassarov and Delépine 2004). We argue that conduction mechanism of quartz is different to that of talc because the content of alkali ions in talc is too small. The electrical conductivity of talc before dehydration is similar to dry minerals such as orthopyroxene (Yang et al. 2011) whose iron content was normalized to the same value as talc used in this study. In addition, a large reduction in water content resulted in the increase in electrical conductivity. Therefore, we conclude that the electrical conductivity of talc is not dominated by proton but by some other defects such as the small polaron, that is, the electron hopping between Fe^{2+} and Fe^{3+}. After dehydration, the activation enthalpy is close that before dehydration, which implies that electrical conductivity is also controlled by small polaron rather than by hydrogen. A possible explanation of the slight increase in electrical conductivity after dehydration is a change in the oxygen fugacity. Upon dehydration decomposition, water released as dehydration reacts with Ni electrode as

$$H_2O + Ni \Leftrightarrow H_2 + NiO$$

The presence of NiO was confirmed after the experiment. Therefore, the oxygen fugacity in the sample assembly must be close to the Ni–NiO buffer. A possible explanation for the increased conductivity is to assume that the starting material was equilibrated with a lower oxygen fugacity than that of the Ni–NiO buffer.

It should be mentioned that Fe or Mg vacancy is an alternative conduction mechanism; however, the activation enthalpy for the diffusion of most of the cations in silicates is on the order of 200–300 kJ/mol (e.g., Brady 1995) which is much higher than that of this study.

Figure 6 also shows a comparison of the electrical conductivity of other hydrous minerals. The measured electrical conductivity of talc before dehydration is slightly lower than the results of Guo et al. (2011) at 3.0 GPa. In contrast, the electrical conductivity of talc above the dehydration temperature is much lower than that of results reported by Zhu et al. (2001). Zhu et al. (2001) argued that dehydration cannot lead to an abrupt increase in electrical conductivity, which is not consistent with our results. In comparison with sheet mineral, for instance, the electrical conductivity of pyrophyllite at 3.5 GPa (Hicks and Secco 1997), containing higher iron content than talc, with activation enthalpy of ~120 kJ/mol, is higher than the present results, suggesting the conduction mechanisms are similar. The electrical conductivity of antigorite with various iron contents given by Reynard et al. (2011) shows very slight differences and is close to that of talc at 0.5 GPa although the iron content in their samples is higher than that of talc. In addition, Reynard et al. (2011) indicated that dominant mechanism of conduction is hopping of small polarons. In

contrast, the electrical conductivity of amphibole-bearing rocks reported by Wang et al. (2012) shows two orders of magnitude higher than that of talc attributed to the significant difference in iron content. The amphibole-bearing rocks studied by Wang et al. (2012) have considerably higher iron content (FeO = 25.44 %) than talc studied in this work. Tolland (1973) reported the electrical conductivity of Mg-rich amphibole with activation enthalpies of 52 kJ along [001] and 55 kJ along [010] and suggested that electrical conductivity is dominated by the electron hopping between Fe^{2+} and Fe^{3+}.

Therefore, we conclude that electrical conductivity of hydrous mineral is likely dominated by ferric iron both before and after dehydration.

MT results show the electrical conductivity in subduction zone is from 10^{-4} to 1 S/m (shown in hatched region). The dehydration of amphibole may yield very high conductivity $\sim$0.1–1.0 S/m. In contrast, the electrical conductivity of hydrous mineral such as talc and antigorite before dehydration remains below 10^{-4} S/m, which cannot explain the high electrical conductivity ($\sim 10^{-2}$–0.5 S/m). However, the ongoing dehydration of talc will enhance electrical conductivity above 0.01 S/m at the very hot areas, which may also provide a clue to explain the high electrical conductivity in certain regions. In addition, attributing high conductivity to talc dehydration would demand deep conductive anomalies (in the subducted lithospheric mantle).For example, most anomalous conductive regions are in the mantle wedge, where hydrous melting is suggested (with hydrous melt conductivity around 1 S/m) by Gaillard (2004), or in the very shallow part where brines are expelled before entering in subduction zones.

We conclude that hydrogen in talc before dehydration does not contribute to electrical conductivity. Rather, electrical conductivity is due mostly to another defect such as ferric iron, Fe^{3+}. However, we should mention that electrical conductivity experiments with variable oxygen fugacity would be helpful to better understand the nature of conduction mechanism of talc in the future. In contrast, in many nominally anhydrous minerals such as olivine and orthopyroxene, the addition of hydrogen significantly enhances electrical conductivity (e.g., Karato and Wang 2012). The observed nearly no role of hydrogen to enhance electrical conductivity in talc (and other hydrous minerals) suggests that only weakly bonded hydrogen enhances electrical conductivity. However, the ongoing dehydration of talc can enhance electrical conductivity in very hot region.

Acknowledgments The authors' thanks Y. Guo, Y. Yu, Z. Liu, D. Li, H. Li and Z. Jiang for their technical assistances. We thank Wyatt L. Du Frane, Fabrice Gaillard and an anonymous reviewer for their constructive comments. This work is partially supported by the important field program of Knowledge innovation Program (KZCX2-YW-QN608) and National Natural Science Foundation of China (NSFC, 40774036) and NSF of USA (EAR-0911465).

References

Bagdassarov NS, Delépine N (2004) α–β Inversion in quartz from low frequency electrical impedance spectroscopy. J Phys Chem Solids 65:1517–1526

Bai L, Conway BE (1991) AC impedance of faradaic reactions involving electrosorbed intermediates: examination of conditions leading to pseudoinductive behavior represented in three-dimensional impedance spectroscopy diagrams. J Electrochem Soc 138:2897–2907

Bailey E, Holloway JR (2000) Experimental determination of elastic properties of talc to 800 °C, 0.5 GPa; calculations of the effect on hydrated peridotite, and implications for cold subduction zones. Earth Planet Sci Lett 183:487–498

Bose K, Ganguly J (1994) Thermogravimetric study of the dehydration kinetics of talc. Am Mineral 79:692–699

Brady JB (1995) Diffusion data for silicate minerals, glasses, and liquids. In: Ahrens TJ (ed) Mineral physics and crystallography: a handbook of physical constants. AGU Reference Shelf, vol 2. Washington, DC, pp 269–290

Evans BW, Guggenheim S (1988) Talc, pyrophyllite, and related minerals. Rev Mineral Geochem 19:225–294

Gaillard F (2004) Laboratory measurements of electrical conductivity of hydrous and dry silicic melts under pressure. Earth Plan Sci Lett 218:215–228

Guo Y, Wang D, Li H, Liu Z, Yu Y (2010) The electrical conductivity of granulite at high temperature and high pressure. Chin J Geophys 53:2681–2687. doi:10.3969/j.issn.0001-5733.2010.11.015

Guo X, Yoshino T, Katayama I (2011) Electrical conductivity anisotropy of deformed talc rocks and serpentinites at 3 GPa. Phys Earth Plan Inter 188:69–81. doi:10.1016/j.pepi.2011.06.012

Helffrich G, Abers GA (1997) Slab low-velocity layer in the eastern Aleutian subduction zone. Geophys J Int 130:640–648

Hicks TL, Secco RA (1997) Dehydration and decomposition of pyrophyllite at high pressures: electrical conductivity and X-ray diffraction studies to 5 GPa. Can J Earth Sci 34:875–882

Huebner JS, Dillenburg RG (1995) Impedance spectra of hot, dry silicate minerals and rock: qualitative interpretation of spectra. Am Mineral 80:46–64

Ichiki M, Baba K, Toh H, Fuji-ta K (2009) An overview of electrical conductivity structures of the crust and upper mantle beneath the northwestern Pacific, the Japanese Islands, and continental East Asia. Gondwana Res 16:545–562. doi:10.1016/j.gr.2009.04.007

Ito K (1990) Effects of H_2O on elastic wave velocities in ultrabasic rocks at 900°C under 1 GPa. Phys Earth Planet Inter 61:260–268

Ito K, Tatsumi Y (1995) Measurement of elastic wave velocities in granulite and amphibolite having identical H_2O free bulk compositions up to 850°C at 1 GPa. Earth Planet Sci Lett 133:255–264

Karato S (1990) The role of hydrogen in the electrical conductivity of the upper mantle. Nature 347:272–273

Karato S, Wang D (2012) Electrical conductivity of minerals and rocks. In: Karato (ed) Physics and chemistry of the deep earth. Wiley-Blackwell (in press)

Kawakatsu H, Watada S (2007) Seismic evidence for deep-water transportation in the mantle. Science 316:1468–1471. doi:10.1126/science.1140855

Kurtz RD, DeLaurier JM, Gupta JC (1990) The electrical conductivity distribution beneath Vancouver Island: a region of active plate subduction. J Geophys Res 95:10929–10949

Liao J, Senna M (1992) Thermal behavior of mechanically amorphized talc. Thermochim Acta 197:295–306

Macdonald D (1978) A method for estimating impedance parameters for electrochemical systems for electrochemical systems that

exhibit pseudoinductance. J Electrochem Soc Solid State Sci Technol 125:2062–2064
Matsuzawa T, Umino N, Hasegawa A, Takagi A (1986) Upper mantle velocity structure estimated from Ps converted wave beneath the north-eastern Japan Arc. Geophys J R Astr Soc 86:767–781
Peacock SM (2001) Are the lower planes of double seismic zones caused by serpentine dehydration in subducting oceanic mantle? Geology 29:299–302
Peacock SM, Hyndman RD (1999) Hydrous minerals in the mantle wedge and the maximum depth of subduction thrust earthquakes. Geophys Res Lett 26:2517–2520
Ranero CR, Morgan JP, McIntosh K, Reichert C (2003) Bending-related faulting and mantle serpentinization at the Middle America trench. Nature 425:367–373
Reynard B, Mibe K, Van de Moortèle B (2011) Electrical conductivity of the serpentinised mantle and fluid flow in subduction zones. Earth Planet Sci Lett 307:387–394. doi:10.1016/j.epsl.2011.05.013
Roberts JJ, Tyburczy JA (1991) Frequency dependent electrical properties of polycrystalline olivine compacts. J Geophys Res 96:16205–16222
Tolland HG (1973) Mantel conductivity and electrical properties of garnet, mica and amphibole. Nature 241:35–36
Ulmer P, Trommsdorff V (1999) Phase relations of hydrous mantle subducting to 300 km, In: Fei et al (eds) Mantle petrology: field observations and high pressure experimentation: a tribute to Francis R. (Joe) Boyd. The Geochemical Society, special publication no. 6, pp 259–281
Wang D, Mookherjee M, Xu Y, Karato S (2006) The effect of water on the electrical conductivity in olivine. Nature 443:977–980
Wang D, Li H, Yi L, Matsuzaki T, Yoshino T (2010) Anisotropy of synthetic quartz electrical conductivity at high pressure and temperature. J Geophys Res 115:B09211. doi:10.1029/2009JB006695
Wang D, Guo Y, Yu Y, Karato S (2012) Electrical conductivity of amphibole-bearing rocks: influence of dehydration. Contrib Mineral Petrol. doi:10.1007/s00410-012-0722-z
Wesolowski M (1984) Thermal decomposition of talc: a review. Thermochim Acta 78:395–421
Yang X, Keppler H, McCammon C, Ni H (2011) Electrical conductivity of orthopyroxene and plagioclase in the lower crust. Contrib Mineral Petrol. doi:10.1007/s00410-011-0657-9
Zhu M, Xie H, Guo J, Xu Z (2001) An experimental study on electrical conductivity of talc at high temperature and high pressure. Chin J Geophys 44:429–435 (in Chinese with English abstract)